Near-surface alignment of polymers in rubbed films

Michael F. Toney*, Thomas P. Russell*, J. Anthony Logan*, Hirotsugu Kikuchi*†, James M. Sands‡ & Sanat K. Kumar‡

* Almaden Research Center, IBM Research Division, 650 Harry Road, San Jose, California 95120, USA
‡ Department of Materials Science and Engineering, The Pennsylvania State University, University Park, Pennsylvania 16802, USA

RUBBED polymer films (generally polyimides) are used in flat-panel displays to control the alignment of liquid crystals in contact with the polymer[1–8], a phenomenon first discovered by Maugin[1] in 1911. Buffing the film with a cloth produces liquid-crystal alignment in the rubbing direction. Several mechanisms have been proposed to explain this effect. The generation of microgrooves or scratches on the polymer surface during rubbing has led to the suggestion that alignment is the result of long-range elastic effects induced by these surface features[3–5]. Others have suggested that the polymer chains near the surface are aligned during rubbing and that these then serve as templates for liquid-crystal alignment[6–13]. Other studies[10–12] have implied that both mechanisms might be operative. Here we present X-ray scattering measurements which show unambiguously that rubbing a polyimide film causes near-surface alignment of the polymer molecules. For a film 200 nm thick, most of the polymer chains within a thin surface region (about 5 nm thick) are aligned in the rubbing direction; for a 6-nm film essentially all of the chains are aligned within 20° of the rubbing direction. This marked orientation of the near-surface chains at temperatures far below the bulk glass transition temperature shows that the mechanical properties of the near-surface region differ significantly from those of the bulk polymer.

Previous studies[6–13] have used bulk-sensitive methods such as optical birefringence and infrared dichroism to infer that rubbing polymer films causes molecular alignment. From measurements as a function of film thickness, it has been suggested that this alignment occurs near the polymer surface[6–8]. Such an interpretation, however, ignores the possibility that the extent of orientation of the polymer depends on film thickness (an effect that our data does in fact show).

To obtain direct information on the effect of rubbing on the near-surface of polyimide films, we have used grazing-incidence X-ray scattering (GIXS)[14–16]. This technique exploits the fact that the index of refraction for X-rays is slightly less than unity; this means that there exists a critical angle, α_c, below which the X-rays are totally externally reflected. Figure 1 illustrates the GIXS geometry. X-rays are incident upon the polymer surface at a grazing angle, α. For $\alpha < \alpha_c$, the X-ray wavefield in the film is evanescent and is limited to the top ~5 nm of the polymer film. The penetration depth of the evanescent field and the projection of the incident beam onto the film surface define a scattering volume that is limited to the near-surface region of the polymer. Conversely, for $\alpha > \alpha_c$, the X-rays penetrate the film to a depth that is limited primarily by their absorption in the material. Therefore, scattering measurements above and below α_c provide a means of distinguishing between the bulk and the near-surface structure of the polymer. In scattering experiments, the intensity of the scattered radiation is determined by structural correlations parallel to the scattering vector **Q** which is the difference between the scattered and incident X-ray wavevectors, **k**′ and **k** (see Fig. 1). The magnitude of **Q** is given by $(4\pi/\lambda)\sin\theta$ where λ is the X-ray wavelength (here 0.1703 nm) and 2θ is the angle between the incident and scattered X-rays. Consequently, measurements of the scattered intensity with **Q** parallel or perpendicular to the rubbing direction permit a determination of the structure parallel or perpendicular to this direction, respectively.

The polyimide used in this study was derived from the polyamic acid ester of bisphenylenedianhydride and *p*-phenylenediamine, denoted BPDA–PDA, and has a quoted[17] glass transition temperature, T_g, in excess of 400 °C. The repeat unit of the polymer is:

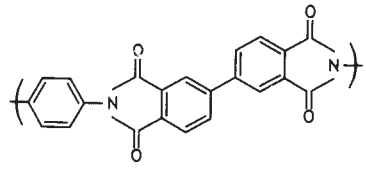

BPDA–PDA films were prepared by spin-coating the precursor poly(amic acid) dissolved in *N*-methylpyrrolidinone onto polished Si(100) wafers. The poly(amic acid) ester was converted to the polyimide by heating the films under N_2 at 5 °C min^{-1} to 250 °C, 300 °C or 400 °C and holding at the specific temperature for 3 h. Films with thicknesses of 6 or 200 nm, as determined by ellipsometry, were investigated. The film thickness was varied by changing the concentration of the solution. Rubbing was performed at room temperature (~20 °C) by pressing the polyimide-coated wafer onto a velour cloth under a load of 2 g cm^{-2} (200 Pa) and unidirectionally pulling the cloth 300 cm at 1 cm s^{-1}. Only the results for films imidized at 300 °C will be reported here, because they are representative of the data for all samples studied.

The upper two curves in Fig. 2 (traces a and b) show the X-ray scattering for a rubbed 200-nm-thick film, with **Q** parallel and perpendicular to the rubbing direction, respectively, where $\alpha > \alpha_c$, that is, the X-rays penetrate the entire film. These data are similar to those reported by others using much thicker specimens[18], and are identical to data from a 200-nm unrubbed film. Thus the rubbing conditions used do not change the bulk structure of the polyimide. The sharp peaks in the scattering profile have been indexed in the figure and arise from the periodic zig-zag of the BPDA–PDA molecules along the chain axis, as shown in the inset. The intensity of these reflections is proportional to the number of BPDA–PDA molecules oriented with their chain axes parallel to **Q**. Also evident in the data are two broad reflections at 13 and 30 nm^{-1} which arise primarily from the intermolecular packing of BPDA–PDA segments normal to the chain axis. The scattering profiles (Fig. 2*a*, *b*) are independent of the sample rotation and, therefore, there is no preferred

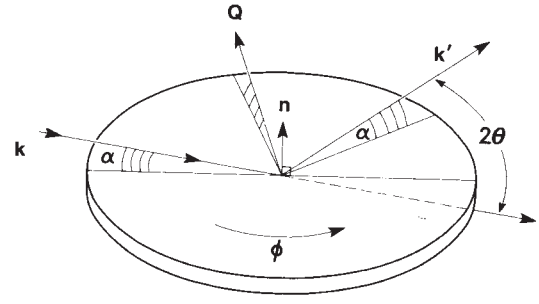

FIG. 1 Grazing-incidence X-ray scattering geometry. The scattering vector **Q** is the difference between the scattered and incident X-ray wavevector and has a magnitude of $(4\pi/\lambda)\sin\theta$, where λ is the X-ray wavelength and θ is one-half of the scattering angle 2θ. The surface normal is **n** and ϕ describes the rotation angle of **Q** with respect to the rubbing direction. The X-ray measurements were conducted on beamline X20C at the National Synchrotron Light Source using a wide bandpass (~1%) synthetic multilayer monochromator.

† Present address; Kyushu University, Fukuoka, Japan.

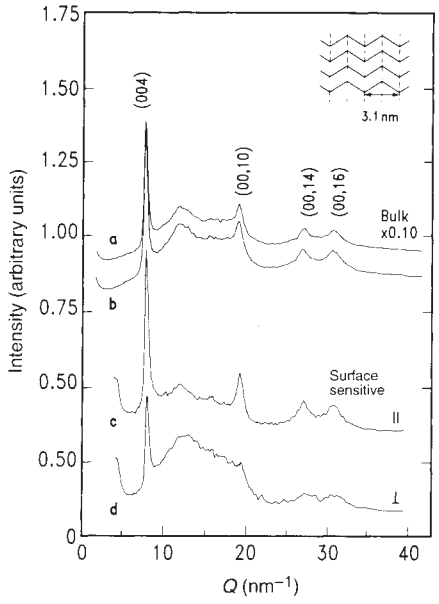

FIG. 2 X-ray scattering intensity (corrected for the illuminated area)[24] for a rubbed 200-nm-thick BPDA–PDA film imidized at 300 °C. Trace a, bulk-sensitive scan ($\alpha > \alpha_c$) for **Q** parallel to the rubbing direction. The labels index the sharp Bragg reflections due to periodic density correlations along the chain axis. Trace b, bulk-sensitive scan ($\alpha > \alpha_c$) for **Q** perpendicular to the rubbing direction. Trace c, surface-sensitive scan ($\alpha = 0.25\alpha_c$) for **Q** parallel to the rubbing direction. Trace d, surface-sensitive scan ($\alpha = 0.25\alpha_c$) for **Q** perpendicular to the rubbing direction. The data have been offset for clarity. Inset, schematic representation of the structural ordering in BPDA–PDA. The dashed lines indicate the periodicity along the chain axis.

alignment of the polymer chains in the bulk of the film under these rubbing conditions.

The lower two scattering profiles in Fig. 2 (traces c and d) were obtained from the near-surface region of the same 200-nm-thick film ($\alpha < \alpha_c$) for **Q** parallel and perpendicular to the rubbing direction, and are denoted as $I_{\parallel}(Q)$ and $I_{\perp}(Q)$, respectively. Two important differences are immediately evident in comparing these profiles. First, the sharp Bragg reflections arising from the periodicity along the BPDA–PDA molecular axes are significantly more intense for $I_{\parallel}(Q)$ than for $I_{\perp}(Q)$. Second, the broad reflections at $Q \approx 13$ and 30 nm^{-1} are much stronger for $I_{\perp}(Q)$ than for $I_{\parallel}(Q)$. This result, coupled with the results from the bulk (Fig. 2*a*, *b*), shows that only in the near-surface region (<5 nm from the surface) do the BPDA–PDA chains orient along the rubbing direction. Quantitatively, twice as many chains in the surface region are aligned parallel to the rubbing direction than are perpendicular, as measured from the intensities of the (004) reflections. Thus our results suggest that it is the oriented chains at the surface that act as a molecular template in aligning the liquid crystals. From the present measurements it is not known whether the near-surface region consists of a thin layer of chains aligned perfectly along the rubbing direction or of patches of thicker, well aligned domains coexisting with more disordered regions. Measurements of $I_{\parallel}(Q)$ and $I_{\perp}(Q)$ as a function of α, which can distinguish between these possibilities, are in progress.

When one considers that the rubbing is done under remarkably small loads (~200 Pa) and at a temperature (20 °C) that is several hundred degrees below the polyimide T_g, it is surprising that the polyimide chains can be oriented at all. This suggests that the yield stress in the near-surface region of the polymer is less than in bulk, due either to a reduction in the number of molecular-chain entanglements near the surface[19] or to a reduction[20–22] in the near-surface T_g. Alternatively, friction may cause the local temperature at the surface to become high enough for a sufficient period of time that the chains can reorient, as discussed by Bowden and Tabor[23]. Experiments are under way to distinguish between these possibilities.

To investigate the effect of film thickness on the molecular orientation, studies were performed on a 6-nm-thick film of BPDA–PDA also imidized at 300 °C. These measurements were done in a GIXS geometry ($\alpha < \alpha_c$) to minimize the background scattering from the Si(100) substrate. Figure 3*a* shows the X-ray scattering for **Q** parallel and perpendicular to the rubbing direction. The absence of any sharp Bragg reflections in the perpendicular profile, and the presence of intense (004) and (00, 10) Bragg reflections in the parallel profile, show that the BPDA–PDA chains are well aligned along the rubbing direction. This is further supported by the strong diffuse reflections at $Q \approx 13$ and 30 nm^{-1} in the perpendicular profile. To quantify further the extent of orientation, the intensity of the (004) reflection was measured as a function of the angle from the rubbing direction and is shown in Fig. 3*b*. It is seen that nearly all the intensity occurs within ±10° of the buffing direction.

As the evanescent wave penetrates most of the 6-nm film, even for $\alpha < \alpha_c$, we conclude that essentially all the BPDA–PDA

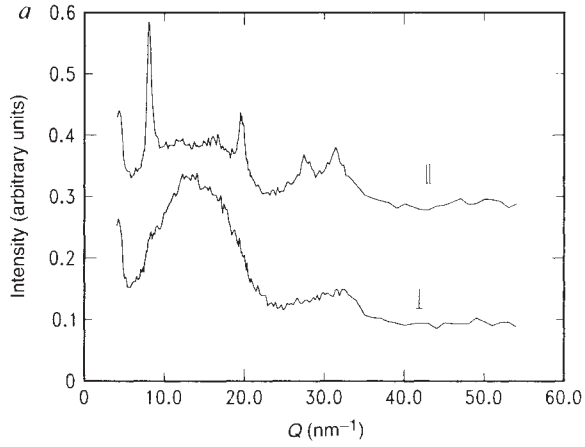

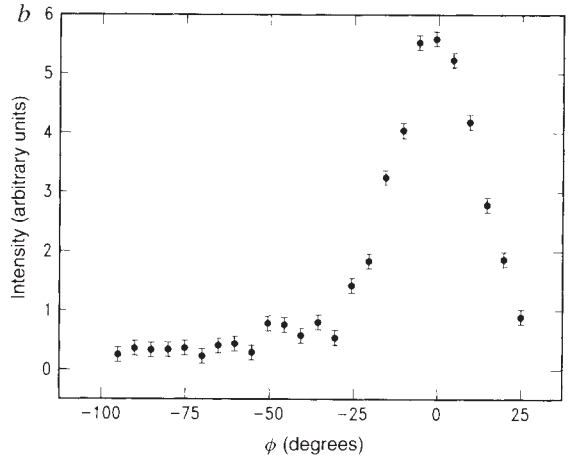

FIG. 3 *a*, X-ray scattering intensity (corrected for the illuminated area)[24] for a 6-nm-thick film of BPDA–PDA imidized at 300 °C. $\alpha = 0.25\alpha_c$ and most of the film is probed by the X-rays. Top trace, **Q** is parallel to the rubbing direction. Bottom trace, **Q** is perpendicular to the rubbing direction. *b*, Intensity of the (004) peak as a function of the angle with respect to the rubbing direction (ϕ in Fig. 1). The data were recorded with the detector at a fixed 2θ while rotating ϕ. The background, corresponding to the average intensity between $Q = 6.0$ and 8.0 nm^{-1}, was subtracted from the peak intensity.

molecules in the film have been oriented with their chain axes parallel to the rubbing direction. This is in marked contrast to the near-surface (<5 nm) region of the 200-nm film, where the chain alignment was significantly less. This difference shows that one cannot reliably use bulk-sensitive measurements (for example, birefringence) as a function of polyimide thickness to infer surface orientation. In addition, the different responses of the 6-nm and 200-nm films to the identical rubbing conditions indicate that either the T_g or the yield stress of the thinner film is lower than that of the near-surface region of the thicker film. This may be attributed to a reduction in the entanglement density which imparts more mobility to the molecules. □

Received 24 October 1994; accepted 7 March 1995.

1. Mauguin, C. *Bull. Soc. fr. Miner.* **34,** 71–76 (1911).
2. Depp, S. W. & Howard, W. E. *Scient. Am.* **268,** 90–97 (1993).
3. Berreman, D. W. *Phys. Rev. Lett.* **28,** 1683–1686 (1972); *Molec. Cryst. liq. Cryst.* **23,** 215–232 (1973).
4. Zhu, Y.-M. *et al. Appl. Phys. Lett.* **65,** 49–51 (1994).
5. Lee, E. S., Vetter, P., Miyashita, T. & Uchida, T. *Jap. J. appl. Phys.* **32,** L1339–L1341 (1993).
6. Castellano, J.-P. *Molec. Cryst. liq. Cryst.* **294,** 33–41 (1983).
7. Geary, J. M., Goodby, J. W., Kmetz, A. R. & Patel, J. S. *J. appl. Phys.* **62,** 4100–4108 (1987).
8. van Aerle, N.A.J.M., Barmentlo, M. & Hollering, R. W. *J. appl. Phys.* **74,** 3111–3120 (1993).
9. van Aerle, N.A.J.M. & Tol, A.J.W. *Macromolecules* **27,** 6520–6526 (1994).
10. Feller, M. B., Chen, W. & Shen, Y. R. *Phys. Rev.* A**43,** 6778–6792 (1991).
11. Chen, W., Moses, O. T., Shen, Y. R. & Yang, K. H. *Phys. Rev. Lett.* **68,** 1547–1550 (1992).
12. Zuang, X., Marucci, L. & Shen, Y. R. *Phys. Rev. Lett.* **73,** 1513–1516 (1994).
13. Kikuchi, H., Logan, J. A. & Yoon, D. Y. *Mater. Res. Soc. Symp. Proc.* **345,** 247–253 (1994).
14. Fuoss, P. H. & Brennan, S. *A. Rev. Mater. Sci.* **20,** 365–390 (1990).
15. Factor, B. J., Russell, T. P. & Toney, M. F. *Macromolecules* **26,** 2847–2859 (1993).
16. Toney, M. F. & Brennan, S. *J. appl. Phys.* **65,** 4763–4768 (1989).
17. Kochi, M., Horigomi, T. & Mita, I. *Recent Advances in Polyimide Science and Technology* 192–200 (eds Weber, W. D. & Gupta, M. R.) (Soc. Plastic Engineering, Poughkeepsie, NY, 1987).
18. Yoon, D. Y., Parrish, W., Depero, L. E. & Ree, M. *Mater. Res. Soc. Symp. Proc.* **227,** 387–393 (1991).
19. Brown, H. R. & Russell, T. P. *Science* (submitted).
20. Reiter, G. *Europhys. Lett.* **23,** 579–584 (1993).
21. Orts, W. J., van Zanten, J. H., Wu, W. L. & Satija, S. K. *Phys. Rev.Lett.* **71,** 87–90 (1993).
22. Keddie, J. L., Jones, R. A. L. & Corey, R. A. *Europhys. Lett.* **27,** 59–64 (1994).
23. Bowden, F. P. & Tabor, D. *The Friction and Lubrication of Solids* Ch. 1 & 2 (Oxford Univ. Press, London, 1950).
24. Toney, M. F. & Wiessler, D. W. *Acta crystallogr.* **49,** 624–642 (1993).

ACKNOWLEDGEMENTS. GIXS measurements were performed at the National Synchrotron Light Source, Brookhaven National Laboratory which is supported by the US Department of Energy. This work was supported, in part, by the US Department of Energy and the US NSF.

Archaean Re–Os age for Siberian eclogites and constraints on Archaean tectonics

D. G. Pearson*†‡, G. A. Snyder§, S. B. Shirey†, L. A. Taylor§, R. W. Carlson† & N. V. Sobolev‖

* Department of Earth Sciences, Open University, Milton Keynes MK7 6AA, UK
† Department of Terrestrial Magnetism, 5241 Broad Branch Road NW, Washington DC 20015, USA
§ Department of Geological Sciences, University of Tennessee, Knoxville, Tennessee 37996, USA
‖ Institute of Mineralogy and Petrography, Siberian Branch, Russian Academy of Sciences, Novosibirsk, Russia

CONSIDERABLE uncertainty surrounds the nature and evolution of the Earth's mantle in Archaean times (>2.5 Gyr ago). Mantle-derived eclogite xenoliths erupted by kimberlites provide important clues in this regard, because their basaltic composition suggests that they may be remnants of an early (>4 Gyr) magma ocean[1,2], subducted Archaean oceanic crust[3–5], or crystallized high-pressure mantle melts[6–9]. Better constraints on the age and origin of mantle eclogites are thus important for our understanding of early Earth processes. Here we present rhenium–osmium isotope data for diamond-bearing eclogites from the Udachnaya kimberlite pipe in Siberia, which indicate formation in the Archaean (2.9 ± 0.4 Gyr). This age is too young for the eclogites to be remnants of early Earth differentiation, but overlaps the age range for crust generation and craton stabilization on both the Aldan and Anabar shields of the Siberian craton (2.85–3.2 Gyr)[10,11]. These data, together with 3.1 Gyr Re–Os model ages for diamond-bearing Udachnaya peridotites[12], show that the Siberian craton lithosphere was at least 150 km thick (the minimum required for diamond stability) by the Mid-Archaean.

A major difficulty with determining the petrogenetic history of mantle eclogites is the lack of definitive age constraints, owing to their complex history[1,2,4]. Here we use the Re–Os isotope system to determine the age of a well-characterized suite of eclogites from the Udachnaya kimberlite pipe in Yakutia, Siberia[13]. The large fractionation of Re from Os during mantle melting produces high, variable Re/Os ratios in magmas which should enable the determination of precise model and isochron ages of ancient magmatic products. Furthermore, the Re–Os isotope system appears less sensitive to the widespread lithospheric metasomatism that severely affects incompatible-element-based isotope systems in Siberian xenoliths[2,12], and hence provides better prospects for dating. For these reasons we have analysed seven well characterized eclogite xenoliths from Udachnaya, six containing diamonds, with the aim of addressing the age and origin of these rocks.

Re and Os contents of the eclogite suite vary from 0.089 to 1.7 p.p.b. and from 0.028 to 0.346 p.p.b. respectively (Table 1). These abundances and the high $^{187}Re/^{188}Os$ values (~12 to >200) differ from komatiites[14,15], a magma type occurring in the Archaean, but span the range of modern[16–18] and Archaean[15] basalts. Osmium isotopic compositions of the Udachnaya eclogites are highly radiogenic, $^{187}Os/^{188}Os = 0.8296$ to 9.808, such that between 10 and 55% of the total Os is from ^{187}Re decay. Thus, Os in the eclogites is considerably more radiogenic than in basalts erupted recently in oceanic settings but is comparable to the present-day isotopic range for magmas erupted in the Archaean (Fig. 1).

To generate the highly radiogenic Os isotopic compositions of the Udachnaya eclogites with their measured Re/Os requires long-term isolation from the convecting mantle. Osmium isotope evolution trajectories for five samples (Fig. 2) show general con-

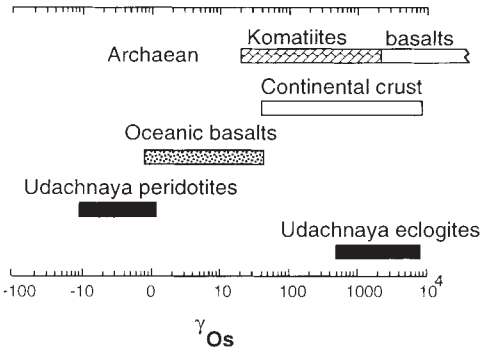

FIG. 1 Osmium isotope composition of Udachnaya eclogites expressed as γ_{Os}. The eclogites are compared to present-day values for Udachnaya peridotites[12], modern oceanic basalts[16–19], continental crust[28] and Archaean komatiites and basalts[14,15].

‡ Present address: Department of Geological Sciences, Durham University, South Road, Durham DH1 3LE, UK.